UV-VIS spectral modifications of water samples under irradiation: lake *vs.* subterranean water.

Silvia Berto,[a] Marco Isaia,[b] Babira Sur,[a,c] Elisa De Laurentiis,[a] Francesco Barsotti,[a] Roberto Buscaino,[a] Valter Maurino,[a] Claudio Minero,[a] Davide Vione [a,d]*

[a] *Università degli Studi di Torino, Dipartimento di Chimica, Via Pietro Giuria 5, 10125 Torino, Italy.* http://www.environmentalchemistry.unito.it

[b] *Università degli Studi di Torino, Dipartimento di Scienze della Vita e Biologia dei Sistemi, Via Accademia Albertina 13, 10123 Torino, Italy.* http://www.personalweb.unito.it/marco.isaia/

[c] *Department of Chemical Engineering, Calcutta University, 92 Acharya P. C. Road, Kolkata 700009, India.*

[d] *Università degli Studi di Torino, Centro Interdipartimentale NatRisk, Via Leonardo da Vinci 44, 10095 Grugliasco (TO), Italy.* http://www.natrisk.org

* Corresponding author. Fax: +39-011-6705242; E-mail: davide.vione@unito.it
URL: http://chimica.campusnet.unito.it/do/docenti.pl/Show?_id=dvione

Abstract

Water samples from subterranean systems (caves and abandoned mines) and from lake epilimnion were optically characterised and irradiated under simulated sunlight, to study the effects that sunlight exposure before sampling may have on the properties and photochemical behaviour of chromophoric dissolved organic matter (CDOM). Differently from lakes, absorption spectra of subterranean water samples showed variations from the typically observed, featureless exponential decay of absorbance *vs.* wavelength. Fluorescence spectra suggested that, compared to lake water and with a single exception, subterranean water had higher proportion of aquagenic/autochthonous CDOM (*e.g.* proteinaceous material) compared to pedogenic/allochthonous one (*e.g.* humic and fulvic substances). Irradiation of subterranean water produced very significant spectral changes, and finally yielded lakewater-like exponential absorption spectra. In contrast, irradiation of lake water produced photobleaching (decrease of the absorbance) but the shapes of absorption spectra underwent very limited variations. Tyrosine and humic acids were irradiated as proxies of the CDOM fractions identified by fluorescence. Irradiated tyrosine underwent a significant increase of the absorbance and finally yielded an exponential absorption spectrum, with close resemblance to the behaviour of a protein-rich and humic-poor sample of subterranean water. In contrast, irradiated humic acids underwent photobleaching in a similar way as lake water, but they retained their typical exponential spectrum. The present findings suggest that exposure of CDOM to sunlight may play a key role in shaping the exponential absorption spectra that are typically observed in surface waters.

Keywords: humic and fulvic acids; photochemistry; phototransformation; UV-Vis spectrophotometry; fluorescence matrix; non-purgeable organic carbon; subterranean environments.

1. Introduction

Chromophoric (or Coloured) Dissolved Organic Matter (CDOM) is the fraction of organic material dissolved in natural waters that is able to absorb radiation. CDOM can be optically characterised by means of its absorption of radiation above 200 nm, although absorption above 250 nm is usually preferred to avoid interference by nitrate [1]. However, from an environmental point of view it is the CDOM ability to absorb sunlight that is most important. CDOM is usually the main radiation absorber in water in the 300-500 nm wavelength interval, and its ability to absorb UVA and UVB radiation has important consequences for aquatic organisms. Indeed, CDOM protects the aquatic biota from exposure to UV radiation [2], which can be very significant during summertime in CDOM-poor environments such as mountain lakes located above the tree-line [3]. Another important issue is that radiation absorption by CDOM yields reactive species, such as $^{\bullet}OH$, $^{1}O_2$ and the triplet states ^{3}CDOM*, which can be involved into transformation of dissolved compounds, including xenobiotics, as well as into the photoprocessing of CDOM itself [4-7].

The absorption spectra of CDOM in surface waters usually show an almost featureless exponential decrease with wavelength, which accounts for the widespread use of the spectral slope S for a qualitative or semi-quantitative description of CDOM characteristics such as molecular weight and aromaticity [8, 9]. Note that S values are obtained by fitting the absorbance (A_λ) spectra of natural waters with the equation $A_\lambda = A_o \cdot e^{-S \cdot \lambda}$. The small deviations of the CDOM spectrum from a purely exponential decay, which can be evidenced by considering the S trend with wavelength ($S(\lambda)$ and/or $\partial S/\partial\lambda$), can be used to differentiate between "different CDOM environments" [10]. However, the amount of knowledge that is presently available is far too limited to enable the full exploitation of $S(\lambda)$ or $\partial S/\partial\lambda$ as tools for CDOM characterisation. Another very useful technique for the study of CDOM is the emission-excitation matrix of fluorescence (EEM). EEM is only capable of detecting fluorophores in CDOM (thus yielding the so-called FDOM, Fluorescent Dissolved Organic Matter), but it is very useful for distinguishing between humic and fulvic substances, proteinaceous material, plankton pigments, and even man-made fluorescent xenobiotics (whitening agents) [11].

Irradiation of CDOM by sunlight causes a decrease of the absorbance (photobleaching), because sunlight-absorbing compounds are often transformed into less absorbing or even non-absorbing ones [12-14]. Photoinduced mineralization (loss of Dissolved Organic Carbon, DOC) can also be observed [15-17]. Interestingly, it has been found that CDOM in subterranean water (groundwater that was collected and irradiated, without pre-exposure to sunlight before sampling) is much more susceptible to photomineralization than CDOM in lake water [18]. A possible explanation is the fact

that groundwater CDOM is shielded from sunlight, which could prevent photolabile species from undergoing phototransformation/mineralization. In contrast, lake water undergoes exposure to sunlight prior to sampling, which could transform photolabile species and cause the remaining CDOM to be rather photostable [18].

This paper reports on a study of spectral CDOM variations upon irradiation under simulated sunlight, comparing lake water samples with samples taken from ponds located in mines and caves. In the latter case, the relevant water as well as its CDOM stayed for prolonged time (months to some years) away from sunlight exposure. The experimental procedures allowed differences to be highlighted, both in the initial samples and in water samples after irradiation.

2. Experimental section

Humic acid sodium salt, L-tyrosine (98%) and H_2O_2 (30%) were purchased from Aldrich. Water samples were collected in ponds present in the studied caves/mines or from the epilimnion of the studied lakes. Table 1 reports sampling sites and dates. The samples, kept in the dark, were transported to the laboratory under refrigeration, vacuum filtered on 0.22 μm cellulose acetate membranes, and stored at 4°C until analysis or irradiation.

Fluorescence measurements were carried out with an Agilent Cary Eclipse fluorescence spectrophotometer. The slit widths were set at 10 nm for both excitation and emission. To obtain fluorescence EEM (Excitation-Emission Matrix) spectra, excitation wavelengths (λ_{ex}) were varied from 210 to 500 nm at 10 nm steps. For each excitation wavelength, the emission (λ_{em}) was detected from 220 to 600 nm at 10 nm steps, using a scanning speed of 600 nm min^{-1} and a photomultiplier voltage of 600 V. The Raman peak of ultra-pure water, obtained with an excitation wavelength of 350 nm, was used as a test for signal stability during measurements. The reported fluorescence spectra are an average of triplicate runs.

The dissolved organic carbon (DOC) was measured as NPOC (Non-Purgeable Organic Carbon) by means of a Shimadzu TOC-V_{CSH} total organic carbon analyser, fed with zero-grade air (SIAD, Bergamo, Italy). For NPOC measurements, before injection, samples were added with 1.5% v/v of 2 M HCl and sparged for 10 min with zero-grade air.

Irradiation experiments were carried out under a solar simulator (Solarbox, manufactured by CO.FO.ME.GRA., Milan, Italy), equipped with a 1500 W Xenon lamp and a 320-nm cut-off filter. Solutions to be irradiated (10 mL total volume) were placed inside cylindrical Pyrex glass cells (4.0 cm diameter, 2.5 cm height) and magnetically stirred during irradiation. The lamp UV irradiance (290-400 nm) on top of the solutions was 30±2 W m^{-2}, measured with a CO.FO.ME.GRA. power metre. The spectral photon flux density of the lamp ($p°(\lambda)$), taken with an Ocean Optics USB2000 CCD spectrophotometer and normalised to actinometry results [18, 19] is reported in Figure 1. Note that 7.3 hours continuous irradiation at that irradiance will deliver the same amount of UV energy per unit surface area, as given by the sun in a fair-weather summer day (*e.g.* 15 July) at 45°N latitude [19]. Conversely, every day (24 h) of irradiation under the lamp would correspond to 3.3

fair-weather summer days. Dark experiments were carried out by wrapping the cells in double aluminium foil, and by placing them under the same lamp adopted for irradiation.

After the scheduled reaction time, absorption spectra of samples were taken by means of a Varian Cary 100 Scan UV-Vis spectrophotometer, adopting Hellma quartz cuvettes with 1 cm optical path length. The measured water spectra are reported as $A_1(\lambda)$ in cm^{-1} units, and are the average of quintuplicate runs. The spectral slope S was determined by fitting the $A_1(\lambda)$ *vs.* λ values with the equation $A_1(\lambda) = A_o\, e^{-S\lambda}$ [20]. The fit interval (280-330 nm) was chosen to ensure a reasonable exponential (or pseudo-exponential) trend of $A_1(\lambda)$ *vs.* λ for all investigated samples and a straightforward comparison of S values among samples. The choice of the wavelength range was limited by sample 3, which showed negligible absorbance above 330 nm.

ESI (Electro Spray Ionization) experiments were conducted with a Thermo Finnigan Advantage Max Ion Trap spectrometer in negative ion mode. Sheath gas flow rate was set at 25 (arbitrary unit), auxiliary gas flow rate at 5 (arbitrary unit), spray voltage at 3.25 kV, capillary temperature at 270 °C, capillary voltage at −7 V, and tube lens offset at −60.00 V. Nitrogen (99.998%, SIAD, Bergamo, Italy) was used as sheath and auxiliary gas.

3. Results and Discussion

3.1. Measurement of DOC and water absorbance

The results of DOC analysis are reported in Table 1. Lake water samples were generally richer in DOC compared to subterranean ones. However, there is the important exception of sample 2 that was collected from a mine pond, which presumably had significant DOC contribution from rotting wooden material that had been used in the past mining activity. The ratio between the absorbance at 254 nm (A_{254nm}) and the DOC can give useful information concerning the origin of CDOM (pedogenic or allochthonous – *e.g.* humic-like material – *vs.* aquagenic or autochthonous) [21]. Table 1 shows that samples 1 and 2 (from abandoned mines rich of rotting wood) have A_{254nm} $DOC^{-1} \geq 0.030$ L (mg C)$^{-1}$ cm^{-1}, not so far from the value of 0.044 L (mg C)$^{-1}$ cm^{-1} observed for fulvic acids [21]. In contrast, sample 3 (from a natural oligotrophic cave) shows a very low A_{254nm} DOC^{-1} value. It would not only suggest the presence of purely autochthonous CDOM, but also of autochthonous CDOM absorbing significantly less than average. Concerning samples A-C, their A_{254nm} DOC^{-1} values are well within the range of typical lake water in NW Italy [22].

3.2. EEM fluorescence spectra

Figure 2 reports the EEM contour plots of investigated water samples. The EEM plots show some linear features, namely the Rayleigh-Tyndall scattering signal ($\lambda_{ex} = \lambda_{em}$) and its second harmonic ($\lambda_{ex} = ½\ \lambda_{em}$), as well as the Raman scattering of water ($\lambda_{ex} < \lambda_{em}$) and its harmonic [23]. Apart from these features that occur in every EEM plot, peaks are present that are peculiar to the fluorescent moieties of CDOM, also termed FDOM. From the peak position, identified by the (λ_{ex},

λ_{em}) couple of values, it is possible to identify different fluorescent substances that may occur in surface waters [11, 24, 25].

Interestingly, all the samples except sample 3 show the presence of very significant amounts of humic-like substances, which are identified from their peak A (λ_{ex} = 210/275 nm, λ_{em} =375/500 nm) and peak C (λ_{ex} = 270/325 nm, λ_{em} = 400/430 nm) [11]. Such peaks are quite high in sample 2, taken from a mine pond characterised by the presence of rotten wood material, which could be a reasonable source of lignin-derived humic substances. Apart from this peculiarity, the peaks of humic-like substances are considerably higher in lake-water samples (A-C) compared to mine (1) or cave (3) ones.

In the case of sample 3, the most important peak is located at λ_{ex} = 220 nm and λ_{em} = 294 nm (it is also observed in the other samples but it is not that prominent). There is also a very small peak that can be attributed to humic-like substances. The former peak is defined as peak T_{UV} in the literature and is accounted for by aromatic amino acids (tryptophan, tyrosine, phenylalanine and the peptides that contain them), as well as by miscellaneous phenolic compounds [11]. Usually, these species are part of the so-called autochthonous organic matter that is produced by in-water biological processes [26]. Overall, EEM spectra confirm the results already obtained with A_{254nm} DOC^{-1}, namely that in sample 3 there is a strong prevalence of aquagenic material over humic or fulvic compounds, while the other samples show a significant contribution from humic substances.

3.3. Irradiation experiments

First of all, it should be observed that irradiation of the studied samples caused no photomineralization, *i.e.* no significant DOC decrease. This finding is in agreement with previous results of irradiation of non-acidified lake water under simulated sunlight [18].

Figure 3A shows the time trends of the absorption spectra of water sample 1 (from an abandoned mine) upon irradiation. An interesting issue of the initial spectrum is the presence of a couple of shoulders around 270 nm and at 310-320 nm. As far as the latter case is concerned, there is literature evidence that it may be caused by material released from plankton [27, 28]. A remarkable feature of sample 1 irradiation was the decrease of the absorbance after three days (photobleaching), followed by a considerable modification of the spectrum shape. Indeed, from about 6 day irradiation onwards the absorption spectrum acquired a typical, featureless quasi-exponential decay with wavelength, which is very often observed in surface waters [29]. For irradiation time ≥ 6 days, photobleaching was detectable but limited. The spectral shape modification is quite interesting. Indeed, a rather atypical initial situation (presence of two shoulders), in a water sample that had evolved in the absence of light, was soon changed by irradiation into a more common scenario. Such a finding might imply that sunlight processing of CDOM could have a role in producing the typical shape of absorption spectra that is usually observed in surface waters.

Figure 3b shows the time trend upon irradiation of the spectral slope *S*, compared with the trend in the dark. Interestingly, a significant decrease of *S* could be detected in the irradiated *vs.* dark

samples, which would imply an increase of CDOM molecular weight and/or aromaticity [9, 21, 30]. This means that the compounds initially present in the sample would be smaller or less aromatic than those formed upon irradiation.

Note that dark evolution of all the studied samples including 1, which could possibly be accounted for by microbiological processes, produced much lower changes in absorption spectra ($A_1(\lambda)$ *vs.* λ) compared to irradiation.

Figure 4a reports the trend of the absorbance *vs.* irradiation time for a mine pond sample (sample n°2), characterised by a rather elevated content of organic matter from decomposition of wood material. The initial spectrum already showed an exponential decay that could be consistent with the occurrence of humic-like species from lignin decomposition. Irradiation caused photobleaching, with limited changes in the spectral shape. Figure 4b shows the time trend of *S* vs. time, under irradiation and in the dark. The spectral slope underwent much smaller changes in sample 2 compared to sample 1, and the *S* values of sample 2 after irradiation were higher than in the dark. This finding implies that irradiation decreased the molecular weight and/or aromaticity of CDOM in sample 2, a result that is not unusual for humic substances [31].

Figure 5a reports the time evolution of $A_1(\lambda)$ upon irradiation of a natural cave sample (n° 3), characterised by low DOC content and low initial absorbance. In addition to featuring very low absorption of radiation, the spectrum of sample 3 significantly departed from an exponential trend. Irradiation for 3 days led to a considerable increase of the absorbance and yielded an absorption spectrum that closely followed an exponential trend. For irradiation times longer than three days, the exponential shape of the spectrum was maintained but photobleaching was observed. Figure 5b reports the time trend of *S*, and shows that the spectral slope significantly decreased upon irradiation. *S* was also lower for the irradiated sample than for the dark one. Molecular weight and aromaticity of CDOM in sample 3 would thus increase upon irradiation, which is a similar behaviour as that of sample 1.

Figures 6-8 report the corresponding time trends of absorption spectra and *S* values for lake water samples (A-C), taken for comparison. In the case of lake water, photobleaching was always observed, with limited changes in the spectra shape. Such behaviour is quite similar to that of mine sample 2 and quite different from the case of samples 1 and 3. The *S* values of A-C were modified upon irradiation, but the differences between the *S* trends of irradiated and dark samples were much lower for lake water than for samples 1 and 3 of subterranean water.

Overall, it appears that the effect of irradiation on the CDOM spectral shape (and, therefore, on its molecular weight/aromaticity) was higher for subterranean than for lake water. Moreover, the irradiation effect on lake water samples was rather uniform (photobleaching, with few changes in spectral shape), while for subterranean samples it was a different issue. First of all, in one case (sample 3) a significant increase of the absorbance was observed rather than photobleaching. Significant changes of spectral shape were then observed for both samples 1 and 3, and irradiation probably produced an increase of the molecular weight and/or aromaticity of CDOM. Even more

interestingly, absorption spectra after irradiation of samples 1 and 3 assumed an exponential-like trend that made them quite similar to lake-water ones.

3.4. Irradiation of model compounds (tyrosine and humic acids)

Figure 9a reports the absorption spectra of a solution containing 1 mM tyrosine + 1 mM H_2O_2, before irradiation and after 60 h irradiation. No change of the tyrosine spectrum was detected in the dark. Hydrogen peroxide was added as source of $^{\bullet}OH$, a reactive species that is photochemically produced by several photosensitisers in surface waters (nitrite, nitrate and most notably CDOM) [18, 30, 32, 33]. Here H_2O_2 was added because it is a rather "clean" $^{\bullet}OH$ source, limiting the formation of additional transients [34].

$$H_2O_2 + h\nu \rightarrow 2\ ^{\bullet}OH \qquad (1)$$

The very significant increase of the absorbance and the resulting exponential spectrum after irradiation suggest the formation of chromophoric species upon irradiation of tyrosine + H_2O_2. It also suggests a very interesting similarity between tyrosine and sample 3 (see Figure 5). The EEM fluorescence spectrum of sample 3 (Figure 2) indicated the presence of protein-like material including aromatic amino-acids, of which tyrosine is a reasonably representative compound. Therefore, it is possible that comparable processes take place in both cases. As far as tyrosine is concerned, literature data suggest that absorbance increase would be accounted for by formation of melanin-like pigments upon tyrosine oxidation [35]. This is a reasonable explanation when considering that the spectral slope S decreased upon irradiation, from 0.24±0.01 nm^{-1} of initial tyrosine to 0.012±0.001 nm^{-1} after 60 h irradiation. Such a remarkable decrease would be connected with a considerable increase of molecular weight, consistent with the formation of oligomeric compounds. The ESI-MS analysis of tyrosine solutions (Figure 10) suggests first of all a fragmentation of tyrosine upon irradiation. The ion with mass/charge ratio m/z = 180 before irradiation would correspond to deprotonated tyrosine (Figure 10a), which is no longer present after 60 h irradiation (Figure 10b). In contrast, the ion with m/z = 117 is probably an extensively oxidised compound that underwent cleavage of the aromatic ring. Indeed, it is quite problematic to assign an aromatic structure of that mass to a compound that could reasonably be formed from tyrosine. No significant ions with m/z < 2000 could be detected (there may be some, but they are very near the background noise, data not reported). This implies that either photogenerated chromophoric compounds had larger mass, or that they underwent very low to negligible ionisation by the ESI(-) source. The use of ESI in positive ion mode did not improve the results.

Figure 9b reports the absorption spectra of 30 mg L^{-1} humic acids (HA), before and after irradiation. Photobleaching is clearly observed, together with a small increase of S from 0.010±0.001 nm^{-1} before irradiation to 0.013±0.001 nm^{-1} after 60 h irradiation. The significant photobleaching is a typical feature of humic acids [36], and makes the studied HA sample quite

similar to humic-rich samples 2 (subterranean water) and A, B, C (lake water). Unfortunately, HA were not ESI-MS amenable, which prevented their *m*/*z* characterization.

Overall, an interesting similarity could be seen between the photochemical behaviour of protein-rich sample 3 and tyrosine, and between humic-rich samples 2, A, B, C and HA. In particular, the formation of chromophoric compounds (possibly melanin-like pigments) upon tyrosine photooxidation, featuring an exponential spectrum may suggest that similar processes could also take place in the protein-rich and humic-poor sample 3.

4. Conclusions

The studied subterranean water samples were quite different from lake water ones. Differences concerned specific absorbance, EEM spectra, and absorption spectral shape. In two out of three cases, the spectral shape of subterranean water was very different from the typical exponential decay with wavelength that was observed in lake water. However, irradiation modified the spectral shape of subterranean water to finally produce an exponential trend. Interestingly, the production of an exponential absorption spectrum in those samples was accompanied by an increase of CDOM molecular weight and/or aromaticity. In contrast, lake water spectra showed photobleaching but underwent more limited variations of spectral slope. It is, therefore, suggested that pre-exposure to sunlight before sampling could play a very significant role in shaping the typically observed exponential spectra of CDOM in surface waters.

Furthermore, a subterranean water sample containing significant amounts of protein-like material, as suggested by EEM fluorescence, underwent considerable absorbance increase upon irradiation. This behaviour was quite similar to that of photo-oxidised tyrosine, also concerning the final exponential shape of the absorption spectrum. In the case of tyrosine, and possibly also of the subterranean sample, the absorbance increase would be due to formation of chromophoric material (possibly melanin-like pigments) upon initial substrate photo-oxidation.

Acknowledgements

SB and MI acknowledge financial support from Compagnia di San Paolo, Torino, Italy (CAVELAB project, line B, area II). Compagnia di San Paolo also supported the post-doc scholarship of BS in Torino (India project). The PhD grant of EDL was financially supported by Progetto Lagrange – Fondazione CRT (Torino, Italy).

References

[1] B. Sulzberger, E. Durisch-Kaiser, Chemical characterization of dissolved organic matter (DOM): A prerequisite for understanding UV-induced changes of DOM absorption properties and bioavailability, Aquat. Sci. 71 (2009) 104-126.

[2] S.L. Cooke, C.L. Williamson, B.R. Hargreaves, D.P. Morris, Beneficial and detrimental interactive effects of dissolved organic matter and ultraviolet radiation on zooplankton in a transparent lake, Hydrobiologia 568 (2006) 15-28.

[3] B. Sonntag, M. Summerer, R. Sommaruga, Factors involved in the distribution pattern of ciliates in the water column of a transparent alpine lake, J. Plankton Res. 33 (2011) 541-546.

[4] S. Canonica, Oxidation of aquatic organic contaminants induced by excited triplet states, Chimia 61 (2007) 641-644.

[5] C. Coelho, G. Guyot, A. Ter Halle, L. Cavani, C. Ciavatta, C. Richard, Photoreactivity of humic substances: relationship between fluorescence and singlet oxygen production. Environ. Chem. Lett. 9 (2011) 447-451.

[6] N.M. Scully, W.J. Cooper, L.J. Tranvik, Photochemical effects on microbial activity in natural waters: the interaction of reactive oxygen species and dissolved organic matter, FEMS Microbiol. Ecol. 46 (2003) 353-357.

[7] J.V. Goldstone, M.J. Pullin, S. Bertilsson, B.M. Voelker, Reactions of hydroxyl radical with humic substances: Bleaching, mineralization, and production of bioavailable carbon substrates, Environ. Sci. Technol. 36 (2002) 364-372.

[8] R. Del Vecchio, N.V. Blough, Spatial and seasonal distribution of chromophoric dissolved organic matter and dissolved organic carbon in the Middle Atlantic Bight, Mar. Chem. 89 (2004) 169-187.

[9] M.D. Scapini, V.H. Conzonno, V.T. Balzaretti, A.F. Cirelli, Comparison of marine and river water humic substances in a Patagonian environment (Argentina), Aquat. Sci. 72 (2010) 1-12.

[10] S.A. Loiselle, L. Bracchini, A.M. Dattilo, M. Ricci, A. Tognazzi, A. Cozar, C. Rossi, Optical characterization of chromophoric dissolved organic matter using wavelength distribution of absorption spectral slopes, Limnol. Oceanogr. 54 (2009) 590-597.

[11] K.M.G. Mostofa, F. Wu, C.Q. Liu, D. Vione, T. Yoshioka, H. Sakugawa, E. Tanoue, Photochemical, microbial and metal complexation behaviour of fluorescent dissolved organic matter in the aquatic environments, Geochem. J. 45 (2011) 235-254.

[12] W.J. De Bruyn, C.D. Clark, L. Pagel, C. Takehara, Photochemical production of formaldehyde, acetaldehyde and acetone from chromophoric dissolved organic matter in coastal waters, J. Photochem. Photobiol. A: Chem. 226 (2011) 16-22.

[13] G.C. Shank, R.G. Zepp, A. Vahatalo, R. Lee, E. Bartels, Photobleaching kinetics of chromophoric dissolved organic matter derived from mangrove leaf litter and floating Sargassum colonies, Mar. Chem. 119 (2010) 162-171.

[14] Y.L. Zhang, M.L. Liu, B.Q. Qin, S. Feng, Photochemical degradation of chromophoric-dissolved organic matter exposed to simulated UV-B and natural solar radiation, Hydrobiologia 627 (2009) 159-168.

[15] G.P. Yang, C.Y. Ren, X.L. Lu, C.Y. Liu, H.B. Ding, Distribution, flux, and photoproduction of carbon monoxide in the East China Sea and Yellow Sea in spring, J. Geophys. Res. 116 (2011) C02001.

[16] C.L. Osburn, L. Retamal, W.F. Vincent, Photoreactivity of chromophoric dissolved organic matter transported by the Mackenzie River to the Beaufort Sea, Mar. Chem. 115 (2009) 10-20.

[17] A. Stubbins, C.S. Law, G. Uher, R.C. Upstill-Goddard, Carbon monoxide apparent quantum yields and photoproduction in the Tyne estuari, Biogeosciences 8 (2011) 703-713.

[18] D. Vione, V. Lauri, C. Minero, V. Maurino, M. Malandrino, M.E. Carlotti, R.I. Olariu, C. Arsene, Photostability and photolability of dissolved organic matter upon irradiation of natural water samples under simulated sunlight, Aquat. Sci. 71 (2009) 34-45.

[19] P.R. Maddigapu, M. Minella, D. Vione, V. Maurino, C. Minero, Modeling phototransformation reactions in surface water bodies: 2,4-Dichloro-6-nitrophenol as a case study, Environ. Sci. Technol. 45 (2011) 209-214.

[20] I. Laurion, M. Ventura, J. Catalan, R. Psenner, R. Sommaruga, Attenuation of ultraviolet radiation in mountain lakes: Factors controlling the among- and within-lake variabilità, Limnol. Oceanogr. 45 (2000) 1274-1288.

[21] J.L. Oliveira, M. Boroski, M., J.C.R. Azevedo, J. Nozaki, Spectroscopic investigation of humic substances in a tropical lake during a complete hydrological cycle, Acta Hydrochim. Hydrobiol. 34 (2006) 608-617.

[22] C. Minero, V. Lauri, G. Falletti, V. Maurino, E. Pelizzetti, D. Vione, Spectrophotometric characterisation of surface lakewater samples: Implications for the quantification of nitrate and the properties of dissolved organic matter, Ann. Chim. (Rome) 97 (2007) 1107-1116.

[23] A. Baker, Fluorescence excitation-emission matrix characterization of river waters impacted by a tissue mill effluent, Environ. Sci. Technol. 36 (2002) 1377-1382.

[24] P.G. Coble, Characterization of marine and terrestrial DOM in seawater using excitation-emission spectroscopy, Mar. Chem. 51 (1996) 325-346.

[25] E. De Laurentiis, M. Minella, V. Maurino, C. Minero, M. Brigante, G. Mailhot, D. Vione, Photochemical production of organic matter triplet states in water samples from mountain lakes, located below or above the treeline, Chemosphere 88 (2012) 1208-1213.

[26] Y.L. Zhang, E.L. Zhang, Y. Yin, M.A. van Dijk, L.Q. Feng, Z.Q. Shi, M.L. Liu, B.Q. Qin, Characteristics and sources of chromophoric dissolved organic matter in lakes of the Yungui Plateau, China, differing in trophic state and altitude, Limnol. Oceanogr. 55 (2010) 2645-2659.

[27] M. Vernet, K. Whitehead, Release of ultraviolet-absorbing compounds by the red-tide dinoflagellate *Lingulodinium polyedra*. Mar. Biol. 127 (1996) 35-44.

[28] Y. Zhang, M.A. van Dijk, M. Liu, G. Zhu, B. Qin, The contribution of phytoplankton degradation to chromophoric dissolved organic matter (CDOM) in eutrophic shallow lakes: Field and experimental evidence, Wat. Res. 43 (2009) 4685-4697.

[29] S.P. Tiwari, P. Shanmugam, An optical model for the remote sensing of coloured dissolved organic matter in coastal/ocean waters, Estuar. Coast. Shelf Sci. 93 (2011) 396-402.

[30] S. Loiselle, D. Vione, C. Minero, V. Maurino, A. Tognazzi, A.M. Dattilo, C. Rossi, L. Bracchini, Chemical and optical phototransformation of dissolved organic matter, Wat. Res. 46 (2012) 3197-3207.

[31] L. Galgani, A. Tognazzi, C. Rossi, M. Ricci, J.A. Galvez, A.M. Dattilo, A. Cozar, L. Bracchini, S.A. Loiselle, Assessing the optical changes in dissolved organic matter in humic lakes by spectral slope distributions, J. Photochem. Photobiol. B-Biol. 102 (2011) 132-139.

[32] F. al Housari, D. Vione, S. Chiron, S. Barbati, Reactive photoinduced species in estuarine waters. Characterization of hydroxyl radicals, singlet oxygen and dissolved organic matter triplet state in natural oxidation processes, Photochem. Photobiol. Sci. 9 (2010) 78-86.

[33] J. Hoigné, Formation and calibration of environmental reaction kinetics: oxidations by aqueous photooxidants as an example, In: W. Stumm (Ed.), Aquatic Chemical Kinetics, Wiley, NY, 1990, pp. 43-70.

[34] P. Nissenson, D. Dabdub, R. Das, V. Maurino, C. Minero, D. Vione, Evidence of the water-cage effect on the photolysis of NO_3^- and $FeOH^{2+}$. Implications of this effect and of H_2O_2 surface accumulation on photochemistry at the air-water interface of atmospheric droplets, Atmos. Environ. 44 (2010) 4859-4866.

[35] M. Fontana, L. Mosca, M.A. Rosei, Interaction of enkephalins with oxyradicals, Biochem. Pharmacol. 61 (2001) 1253-1257.

[36] L. Galgani, A. Tognazzi, C. Rossi, M. Ricci, J.A. Galvez, A.M. Dattilo, A. Cozar, L. Bracchini, S.A. Loiselle, Assessing the optical changes in dissolved organic matter in humic lakes by spectral slope distributions, J. Photochem. Photobiol. B: Biol. 102 (2011) 132-139.

Table 1. Features of the studied lake and subterranean water samples. The error bounds represent ±σ of runs carried out at least in quadruplicate on different aliquots of the same sample.

Sample acronym	**Sample source**	**Location Municipality (Province)**	**Coord UTM**	**Sampling date**	**DOC, mg C L^{-1}**	**IC, mg C L^{-1}**	**A_{254nm} DOC^{-1}, L cm^{-1} (mg C)$^{-1}$**
1	Abandoned Talc Mine Santa Barbara	Prali (Torino)	32T 348074 4977205	26 Mar 2010	1.28±0.02	27.2±0.3	0.037±($6\cdot10^{-4}$)
2	Abandoned Talc Mine Gianfranco	Prali (Torino)	32T 348059 4977358	26 Mar 2010	2.75±0.05	74.7±0.6	0.030±($5\cdot10^{-4}$)
3	Barôn Litrôn Cave	Valdieri (Cuneo)	32T 373117 4902365	25 Apr 2010	0.58±0.02	24.6±0.2	0.006±($2\cdot10^{-4}$)
A	Candia Lake	Candia (Torino)	32T 414676 5019591	22 Sep 2010	5.74±0.11	16.5±0.2	0.014±($3\cdot10^{-4}$)
B	Avigliana Lake (Grande)	Avigliana (Torino)	32T 372999 4991538	13 Jun 2010	3.28±0.03	49.1±0.2	0.020±($2\cdot10^{-4}$)
C	Laghetto Lake	Coazze (Torino)	32T 357492 4989084	18 Jun 2010	1.30±0.05	1.45±0.01	0.025±0.001

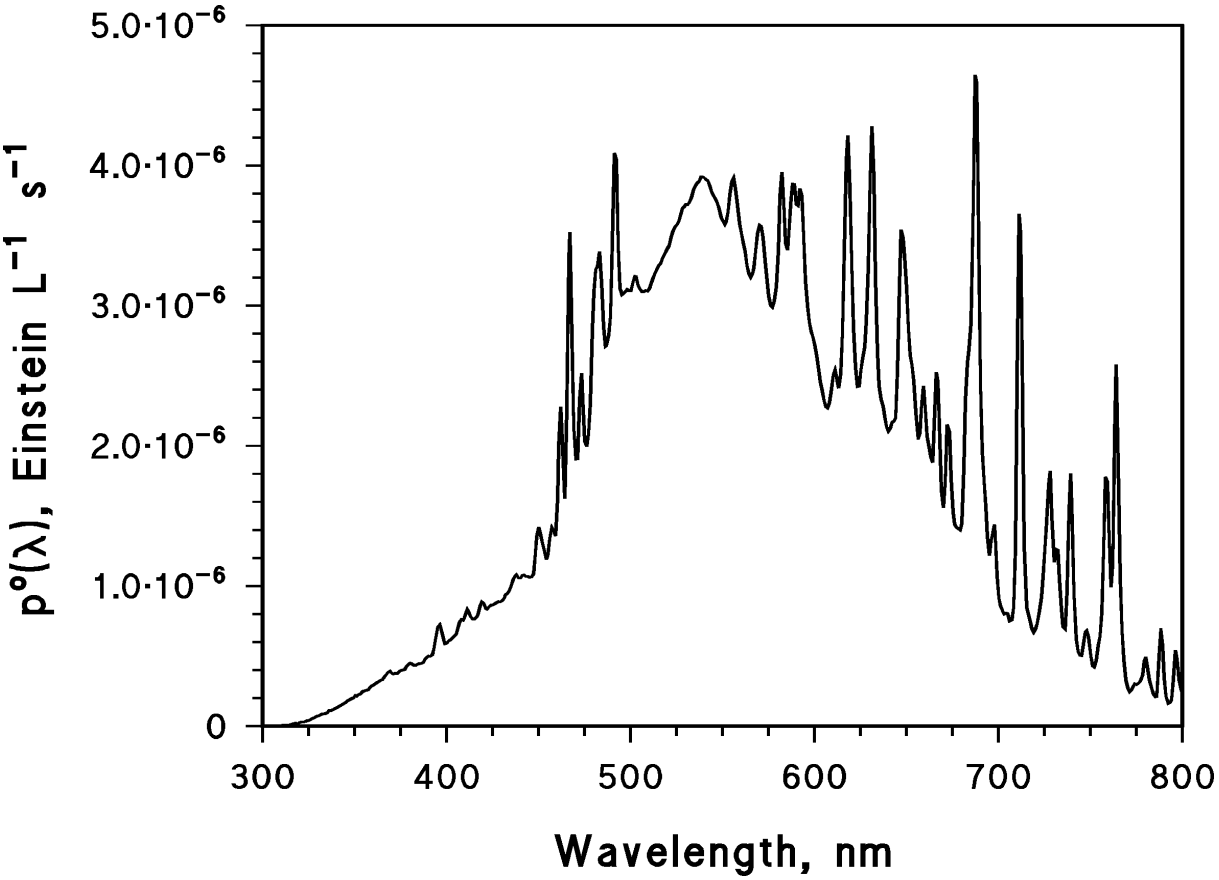

Figure 1. Spectral photon flux density ($p°(\lambda)$) of the adopted solar simulator.

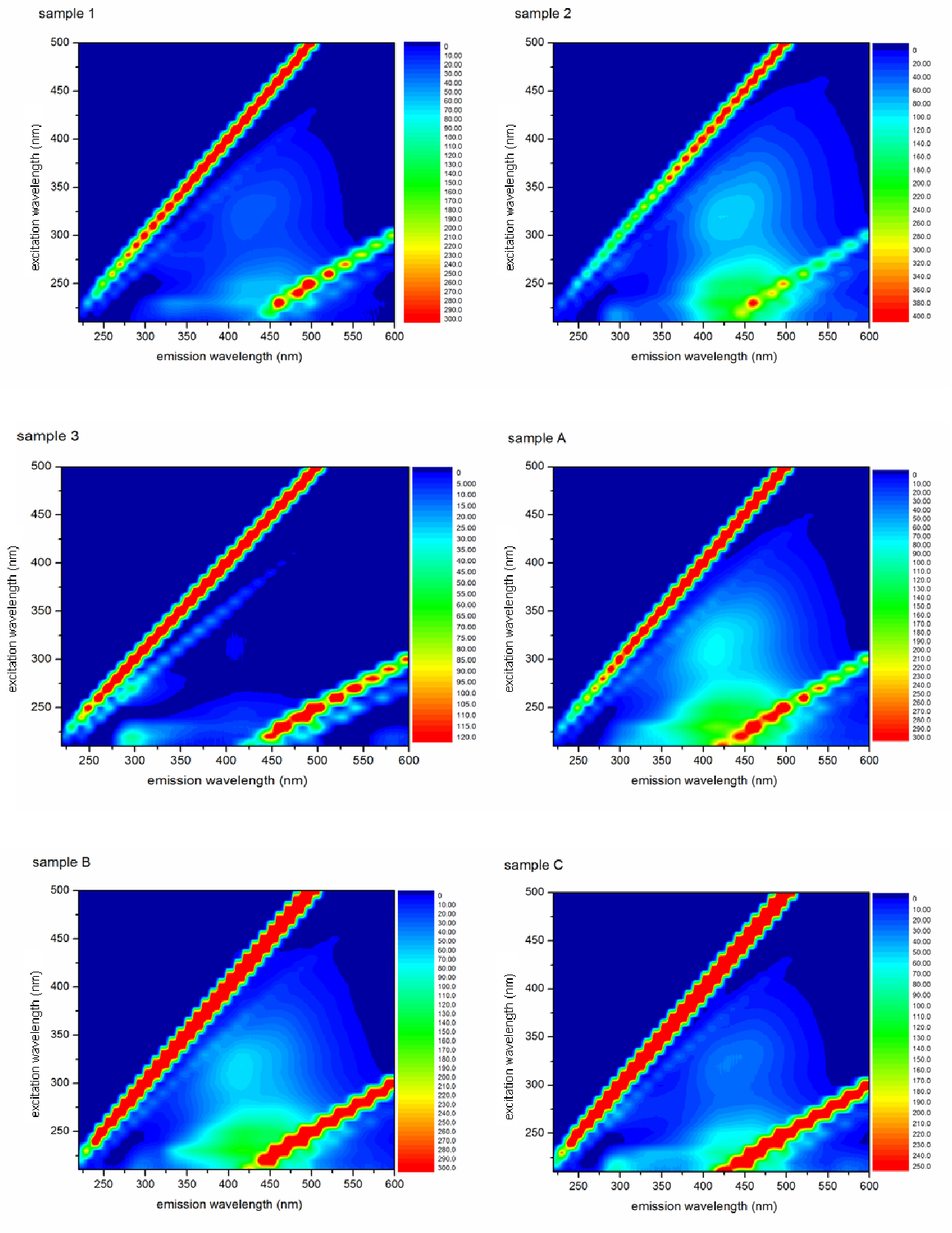

Figure 2. Excitation-emission matrix (EEM) spectra of the studied subterranean water (1-3) and lake water (A-C) samples.

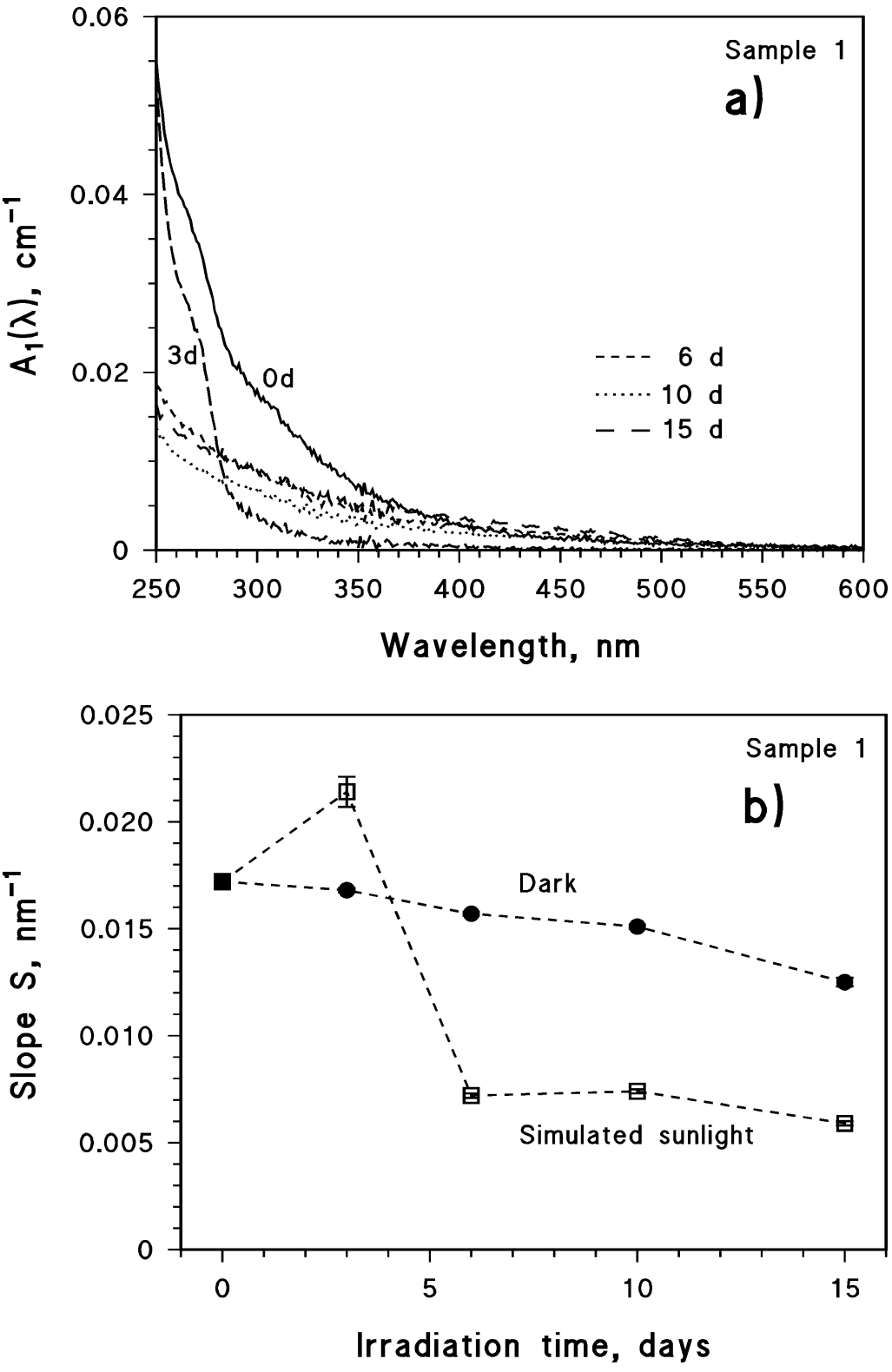

Figure 3. a) Trend of the absorption spectrum of sample 1 (abandoned mine) with irradiation time, under simulated sunlight.

b) Trend of the spectral slope *S* of sample 1, upon irradiation under simulated sunlight as well as in the dark.

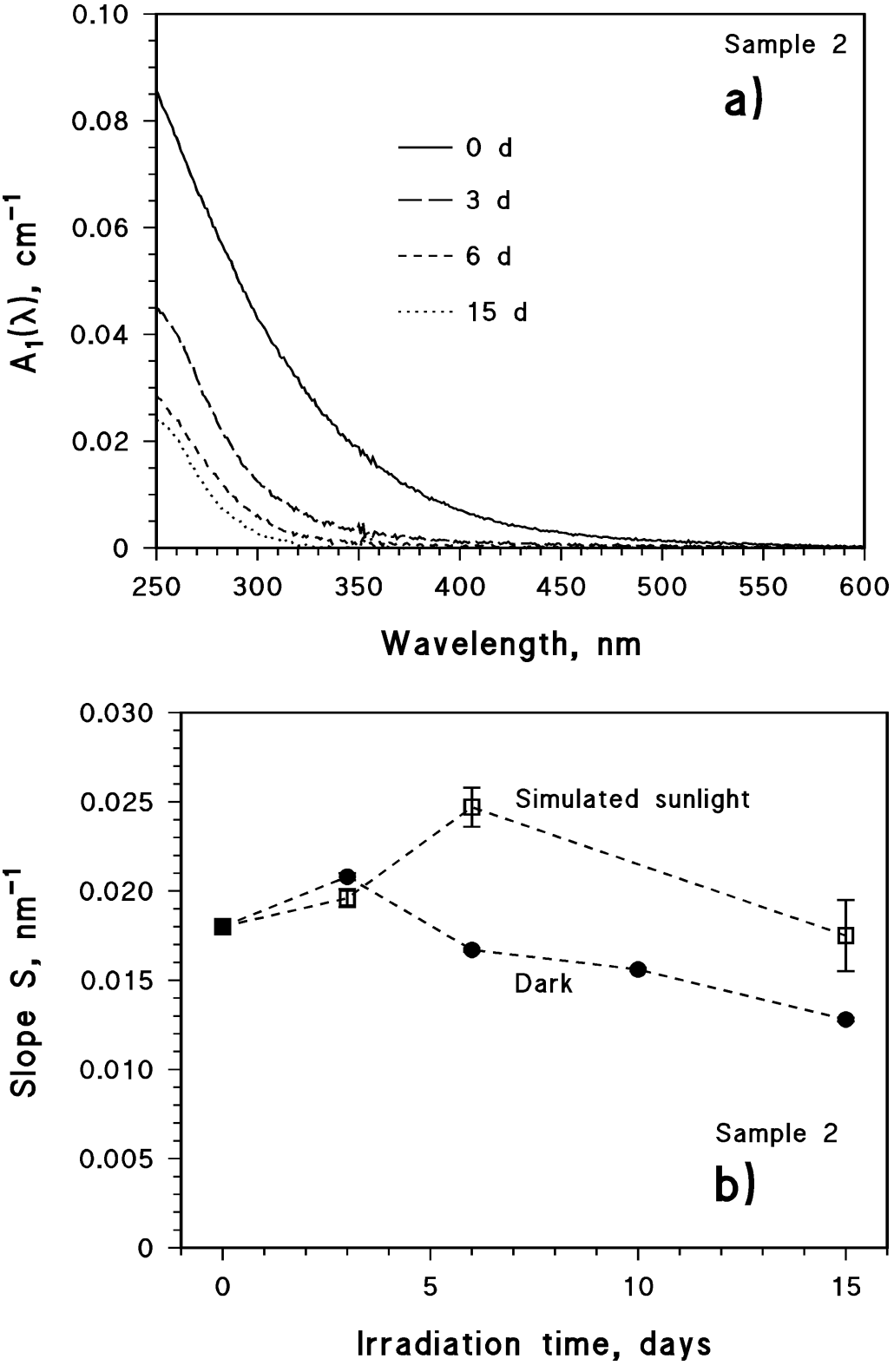

Figure 4. a) Trend of the absorption spectrum of sample 2 (abandoned mine) with irradiation time, under simulated sunlight.

b) Trend of the spectral slope *S* of sample 2, upon irradiation under simulated sunlight as well as in the dark.

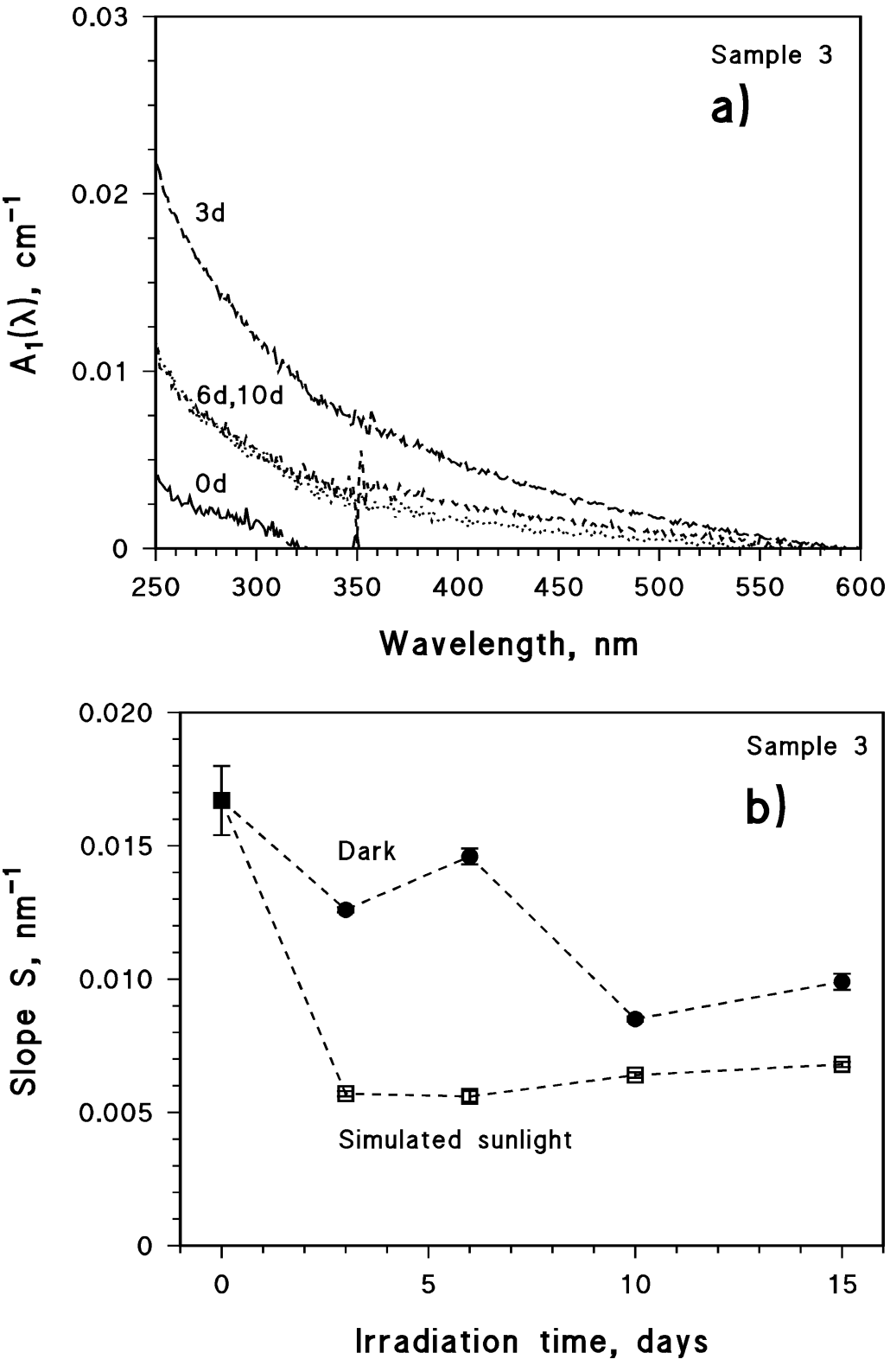

Figure 5. a) Trend of the absorption spectrum of sample 3 (cave) with irradiation time, under simulated sunlight.

b) Trend of the spectral slope *S* of sample 3, upon irradiation under simulated sunlight as well as in the dark.

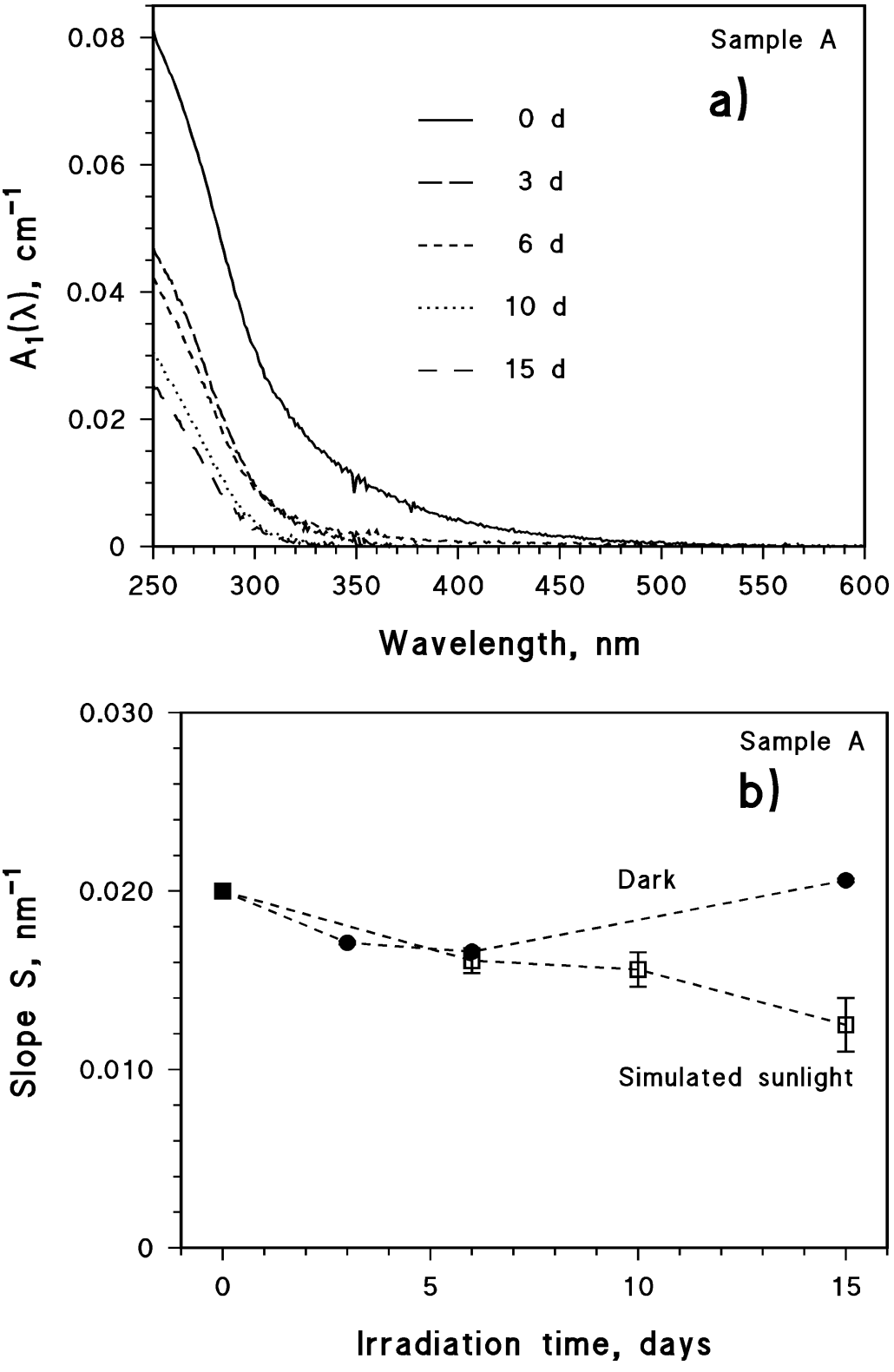

Figure 6. a) Trend of the absorption spectrum of sample A (lake Candia) with irradiation time, under simulated sunlight.

b) Trend of the spectral slope *S* of sample A, upon irradiation under simulated sunlight as well as in the dark.

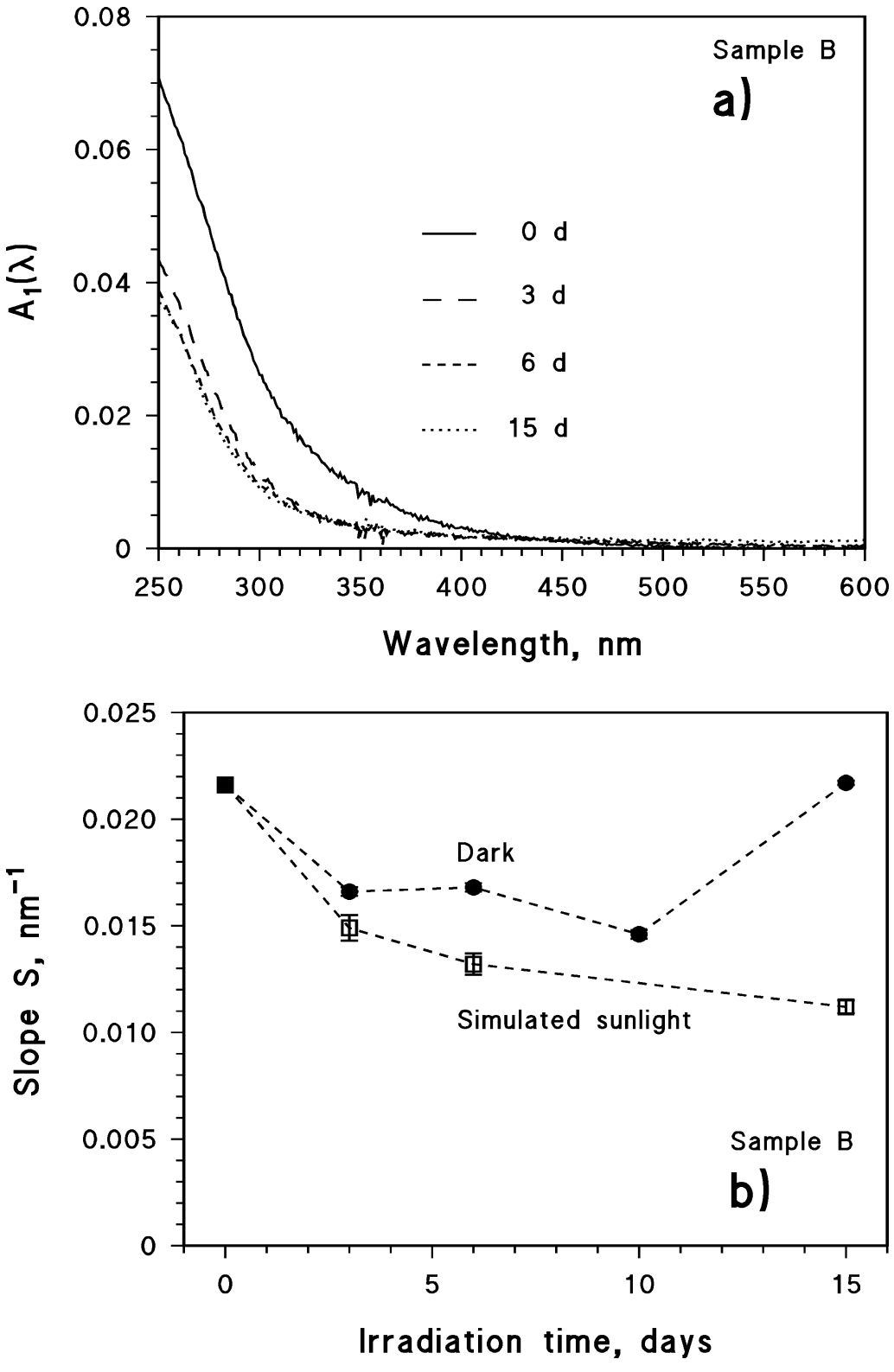

Figure 7. a) Trend of the absorption spectrum of sample B (lake Avigliana) with irradiation time, under simulated sunlight.

b) Trend of the spectral slope *S* of sample A, upon irradiation under simulated sunlight as well as in the dark.

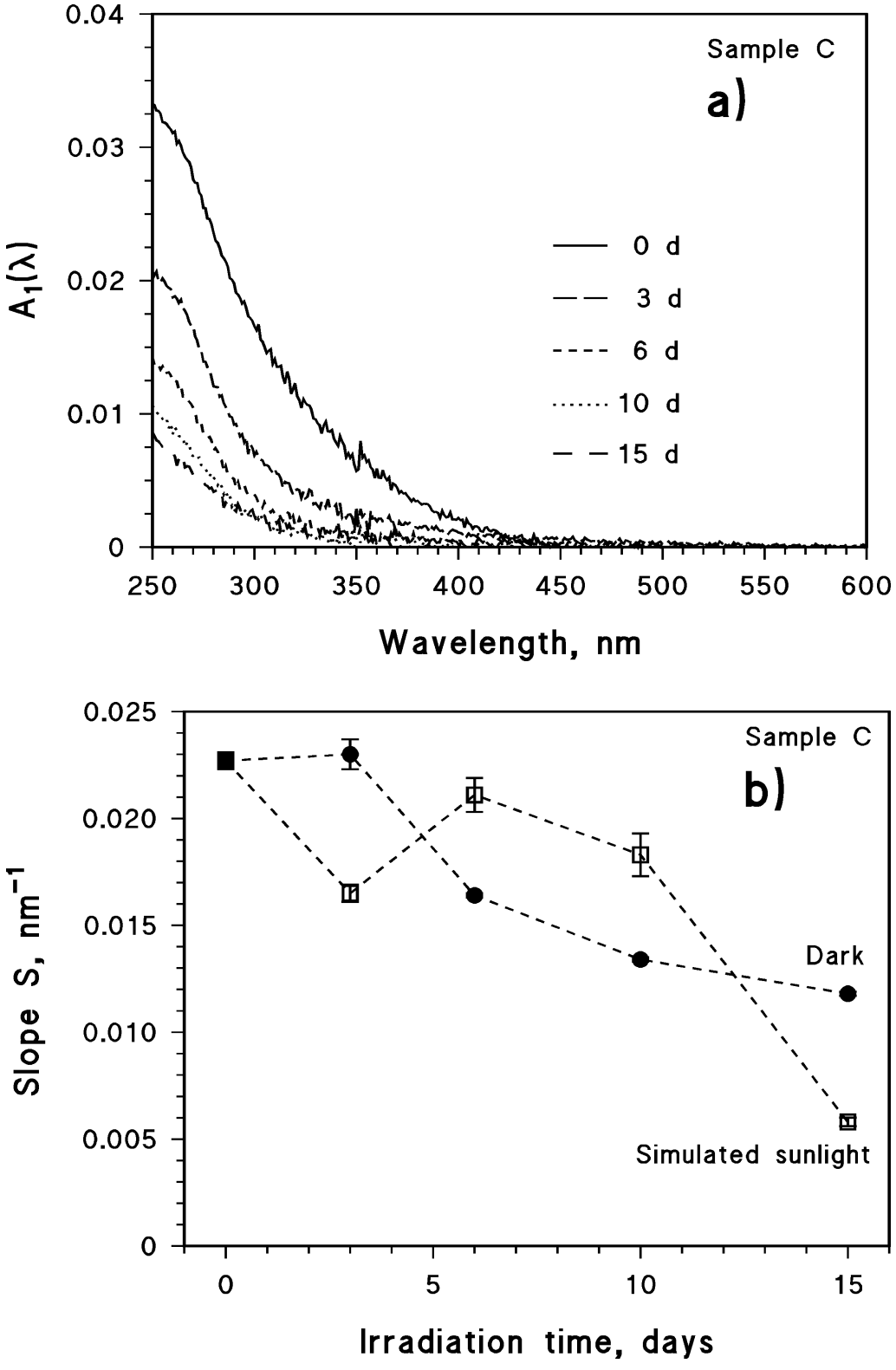

Figure 8. a) Trend of the absorption spectrum of sample C (lake Laghetto) with irradiation time, under simulated sunlight.

b) Trend of the spectral slope *S* of sample C, upon irradiation under simulated sunlight as well as in the dark.

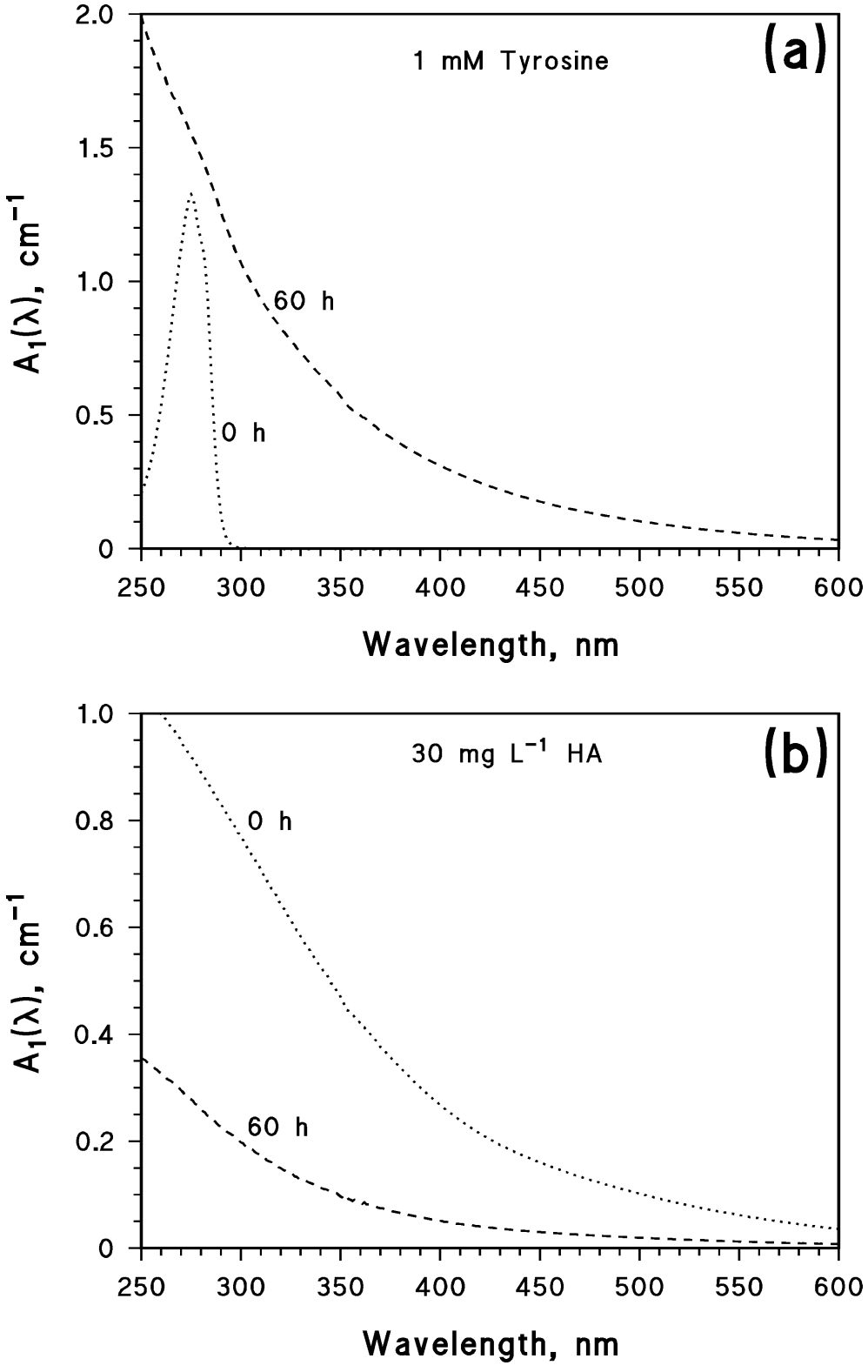

Figure 9. a) Absorption spectrum of 1 mM tyrosine + 1 mM H_2O_2, before and after irradiation.
b) Absorption spectrum of 30 mg L^{-1} humic acids, before and after irradiation.

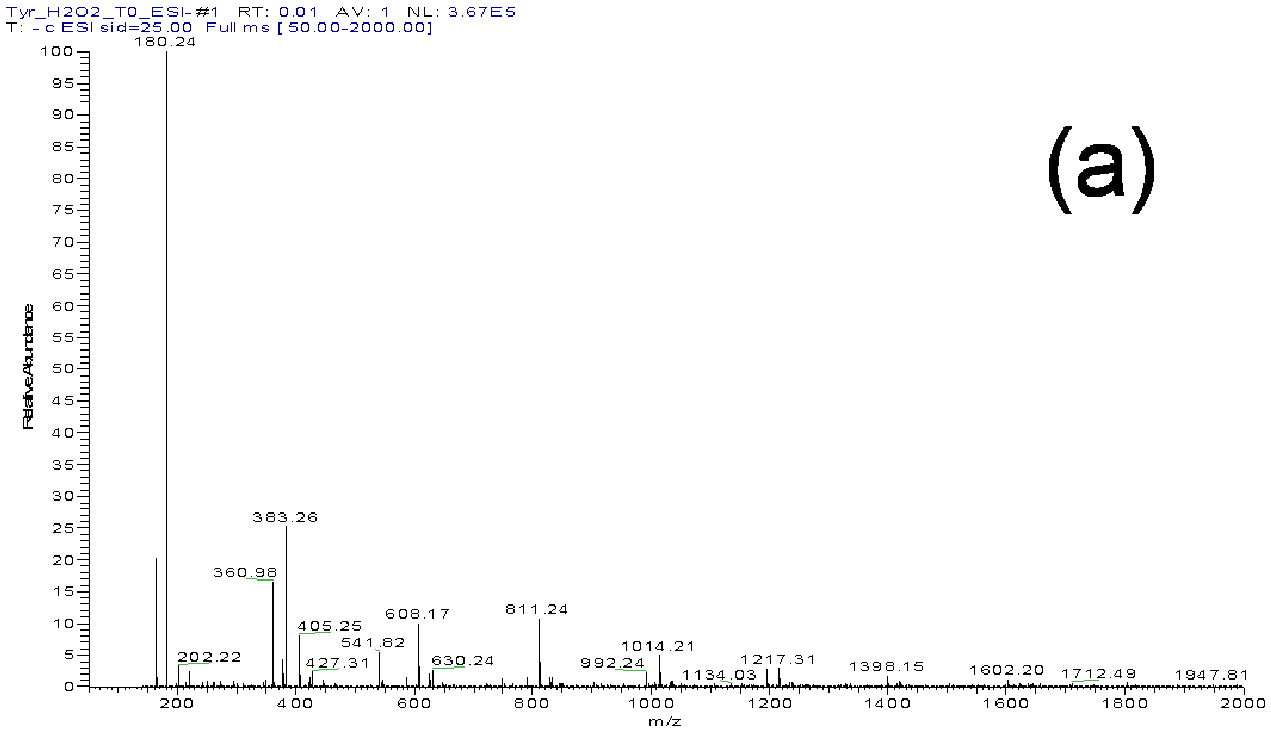

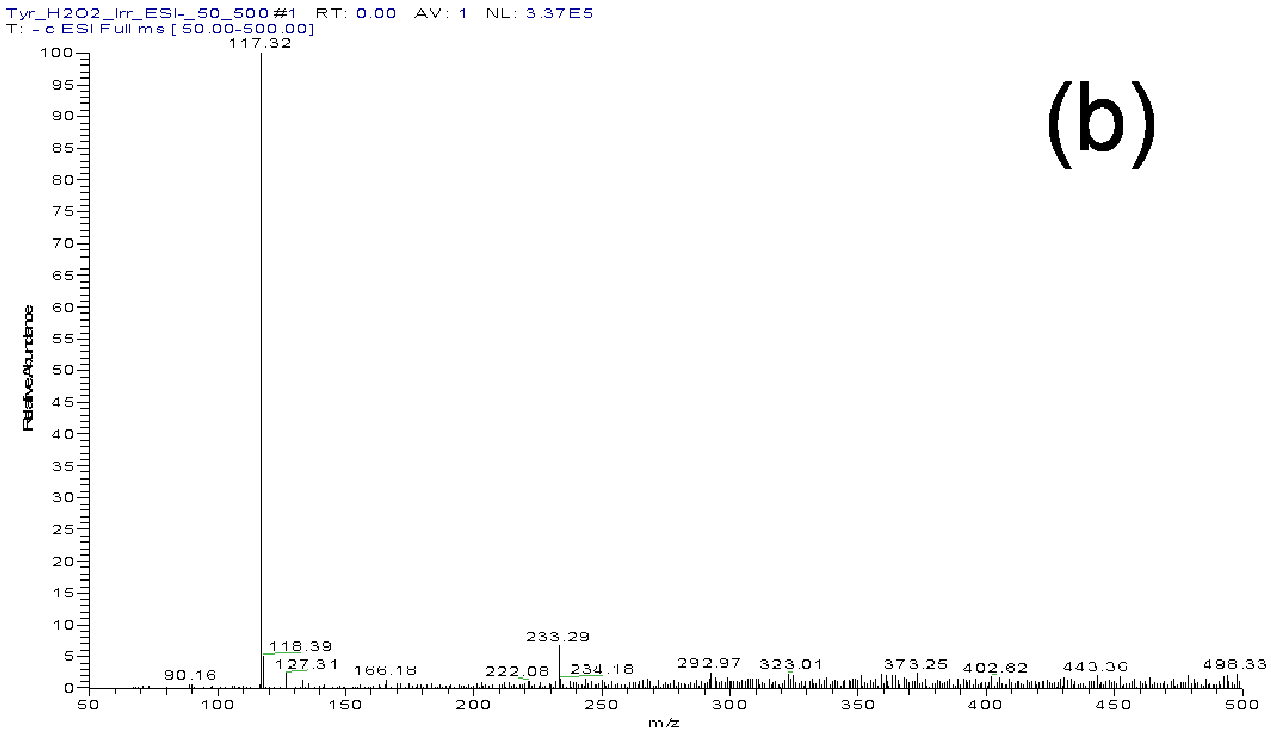

Figure 10. a) ESI(-)-MS spectrum of 1 mM tyrosine + 1 mM H_2O_2, before irradiation.
b) ESI(-)-MS spectrum of 1 mM tyrosine + 1 mM H_2O_2 after irradiation.